

Octahedral As in M^+ arsenates – architecture and seven new members

Karolina Schwendtner* and Uwe Kolitsch

Institut für Mineralogie und Kristallographie,
Universität Wien, Althanstrasse 14, 1090 Wien,
AustriaCorrespondence e-mail:
karolina.schwendtner@univie.ac.atReceived 12 July 2006
Accepted 18 December 2006

Arсенates with arsenic in octahedral coordination are very rare. The present paper provides an overview of all known M^+ arsenates(V) containing octahedrally coordinated arsenic ($M^+ = \text{Li, Na, K, Rb, Cs, Ag}$) and the crystal structures (determined from single-crystal X-ray diffraction data) of the following seven new hydrothermally synthesized members belonging to six different structure types, four of which are novel: $\text{LiH}_2\text{As}_3\text{O}_9$, $\text{LiH}_3\text{As}_2\text{O}_7$, NaHAS_2O_6 -type KHAS_2O_6 , $\text{KH}_3\text{As}_4\text{O}_{12}$ and isotypic $\text{RbH}_3\text{As}_4\text{O}_{12}$, CsAs_3O_8 and $\text{NaH}_2\text{As}_3\text{O}_9$ -type $\text{AgH}_2\text{As}_3\text{O}_9$. The main building unit of these compounds is usually an As_4O_{14} cluster of two edge-sharing AsO_6 octahedra sharing two apical corners each with two AsO_4 tetrahedra. The different connectivity between these clusters defines the different structure types. The novel CsAs_3O_8 structure, based on a derivative of the As_4O_{14} cluster, is the most condensed of all these M^+ arsenates, with an O/As ratio of only 2.67 compared with values of 2.75–3.5 for the remaining members. This is achieved through polymerization of the cluster derivatives to infinite chains of edge-sharing AsO_6 octahedra. The $^{[4]}\text{As}/^{[6]}\text{As}$ ratio drops to only 0.5. All but two of the protonated title compounds show protonated AsO_6 octahedra. Hydrogen bonds range from very strong to weak. An analysis of bond-length distribution and average bond lengths in AsO_6 octahedra in inorganic compounds leads to an overall mean As–O distance for all known AsO_6 octahedra (with R factors < 0.072) of 1.830 (2) Å.

1. Introduction

Extensive studies of the system $M^+ - M^{3+} - \text{As} - \text{O} - \text{H}$ ($M^+ = \text{Li, Na, K, Rb, Cs, Ag, Tl, NH}_4$; $M^{3+} = \text{Al, Ga, In, Sc, Cr, Fe}$) have yielded a large number of new $M^+ - M^{3+}$ arsenates(V) (Kolitsch, 2004; Kolitsch & Schwendtner, 2004, 2005; Schwendtner & Kolitsch, 2004*a,b*, 2005*a,b,c*, 2007*a,b*; Baran *et al.*, 2006*a,b*; Schwendtner, 2006; Schwendtner *et al.*, 2006*a,b,c*), which were characterized structurally but also by spectroscopic and thermoanalytical techniques. As by-products in some of these studies six novel M^+ arsenates(V) were obtained that all contain arsenic in both octahedral and tetrahedral coordination. It is our aim to structurally characterize these materials and have a closer look at AsO_6 units in M^+ arsenates in general. A large number of M^+ arsenates(V) is known, demonstrated by 53 entries in the Inorganic Crystal Structure Database (ICSD, Version 2006-1), most of them featuring arsenic in tetrahedral coordination. All of the 15 (NH_4) arsenates in the database contain only tetrahedrally coordinated arsenic, as do ten out of 13 Na arsenates; these two systems seem to have been studied most extensively. Two of seven Ag arsenates contain AsO_6 octahedra, as does one of

Table 1

Unit-cell parameters of all known M^+ arsenates containing As in octahedral coordination.

Formula	Space group	<i>a</i> (Å)	<i>b</i> (Å)	<i>c</i> (Å)	α (°)	β (°)	γ (°)	<i>V</i> (Å ³)	<i>Z</i>
LiAsO ₃ ^a	$R\bar{3}$	4.808 (3)	4.808 (3)	14.21 (2)	90.00	90.00	120.00	284.48	6
LiH ₂ As ₃ O ₉ ^b	$P2_1/n$	9.666 (2)	8.553 (2)	9.970 (2)	90.00	117.86 (3)	90.00	728.7 (3)	4
LiH ₃ As ₂ O ₇ ^b	$C2/m$	11.456 (2)	9.133 (2)	5.630 (1)	90.00	115.56 (3)	90.00	531.4 (2)	4
Na ₂ As ₄ O ₁₁ ^c	$C2/c$	9.049 (3)	8.287 (3)	11.508 (5)	90.00	102.74 (4)	90.00	842 (2)	4
Na ₇ As ₁₁ O ₃₁ ^d	$P\bar{3}m1$	11.199 (3)	11.199 (3)	5.411 (2)	90.00	90.00	120.00	587.80 (3)	1
NaHAS ₂ O ₆ ^e	$P2_1/c$	5.829 (1)	9.154 (1)	8.989 (1)	90.00	93.29 (1)	90.00	478.85	4
NaH ₂ As ₃ O ₉ ^f	$P\bar{1}$	7.167 (1)	7.575 (1)	7.850 (1)	109.89 (1)	107.27 (1)	106.15 (1)	346.9	2
Na ₃ H ₅ As ₄ O ₁₄ ^g	$Pnna$	10.038 (1)	11.692 (2)	9.533 (1)	90.00	90.00	90.00	1118.83	4
KHAS ₂ O ₆ ^b	$P2_1/c$	6.051 (1)	9.727 (2)	9.054 (2)	90.00	94.21 (3)	90.00	531.46 (18)	4
KH ₃ As ₄ O ₁₂ ^b	$P\bar{1}$	5.154 (1)	6.967 (1)	7.532 (2)	63.90 (3)	78.61 (3)	84.35 (3)	238.08 (11)	1
RbH ₃ As ₄ O ₁₂ ^b	$P\bar{1}$	5.169 (1)	7.036 (1)	7.766 (2)	63.31 (3)	79.87 (3)	84.38 (3)	248.36 (11)	1
CsAs ₃ O ₈ ^b	$C2/c$	8.515 (2)	11.690 (2)	7.595 (2)	90.00	112.70 (3)	90.00	697.5 (3)	4
AgAsO ₃ ^h	$Pca2_1$	19.488 (3)	6.600 (1)	12.661 (3)	90.00	90.00	90.00	1628.47	24
AgH ₂ As ₃ O ₉ ^b	$P\bar{1}$	7.162 (1)	7.678 (2)	7.880 (2)	110.72 (3)	106.47 (3)	105.43 (3)	354.8 (2)	2
Ag ₄ H ₄ As ₄ O ₁₄ ⁱ	$P2_1/n$	7.839 (5)	12.428 (5)	6.556 (2)	90.00	109.30 (2)	90.00	602.81	2

References: (a) Driss & Jouini (1989a); (b) this work; (c) Driss, Jouini & Omezzine (1988); (d) Guesmi *et al.* (2006); (e) Nguyen Huy & Jouini (1978); (f) Driss, Jouini, Durif & Averbuch-Pouchot (1988); (g) Driss & Jouini (1989b); (h) Curda *et al.*, 2004; (i) Boudjada & Averbuch-Pouchot (1984).

the six Li compounds, but none of all six K arsenates. None of the three Tl compounds, the two Cs compounds and the single Rb arsenate contain AsO₆ octahedra. It is interesting to note that octahedrally coordinated arsenic is never encountered together with H₂O in any of these structures. Altogether, there are only seven out of 53 entries featuring the rather rare octahedral coordination of arsenic. An overall analysis of all AsO₄ and AsO₆ polyhedra in structures included in the ICSD leads to the conclusion that only ca 3% of all As^V-containing structures feature the AsO₆ polyhedra (Schwendtner, 2007). To our knowledge an analysis and discussion of bond-length distribution and average bond lengths of AsO₆ groups has never been conducted – probably due to the meagre amount of data. Therefore, a bond-length analysis of all AsO₆ bond lengths available in the ICSD was conducted.

The present paper describes the crystal structures of seven new Li, K, Rb, Cs and Ag arsenates containing arsenic in octahedral coordination, and provides an overview on the topology and connectivity of all M^+ arsenates containing AsO₆ octahedra (Table 1).

2. Experimental

2.1. Syntheses

Six of the seven new compounds were initially synthesized by chance as by-products during the syntheses of M^+-M^{3+} arsenates. Five of these seven compounds were later also obtained in relatively large percentages from M^+-As mixtures (see below). All syntheses were undertaken under hydrothermal conditions in Teflon-lined stainless steel autoclaves at 493 K under autogeneous pressure. The Teflon vessels were filled to ca 30–50% of their inner volume and were then heated to 493 K, kept at this temperature for 7 d, and slowly cooled to room temperature overnight. Powders of M^{2+} CO₃ (purities > 99, 99.5, 99.7, 99.9% for $M^+ = Li, K, Ag,$ and Rb, Cs, respectively), crystalline arsenic acid (H₃AsO₄·0.5H₂O, purity > 99.9%) and (initially) M_2^{3+} O₃/Cr^{III}(NO₃)₃·9H₂O were used as starting reagents. We point out that all of the crystals were

grown without any added water. Four of the seven compounds could be grown from synthesis batches containing either $M_2^+CO_3$, $M_2^{3+}O_3$ and arsenic acid or $M_2^+CO_3$ and arsenic acid only. Two compounds formed only as by-products during the synthesis of M^+-M^{3+} arsenates, while one compound was only obtained by direct synthesis from $M_2^+CO_3$ and arsenic acid.

Colourless to white rhombic crystals of LiH₂As₃O₉ appeared repeatedly in different dry synthesis batches of Li₂CO₃, In₂O₃ and H₃AsO₄·0.5H₂O (volume ratio ca 2:1:6). The yield of the hygroscopic crystals was ca 90%. The same crystals were also obtained from similar mixtures with different M^{3+} cations (Cr, Fe, Sc). Small crystals of LiH₂As₃O₉ (yield ca 40%, accompanied by 60% of amorphous unidentified material) were also grown from a mixture of Li₂CO₃ and arsenic acid (volume ratio ca 1:3) and from the same starting reagents (volume ratio ca 1:2), this time accompanied by crystals of LiAsO₃ (Driss & Jouini, 1989a).

Block, whitish crystals of LiH₃As₂O₇ were found in a dry mixture of Li₂CO₃, In₂O₃ and arsenic acid (volume ratio ca 4:1:5); yield about 50%. The crystals were accompanied by colourless hexagonal platelets of LiAsO₃ (Driss & Jouini, 1989a) and colourless mica-like twinned rosettes of a compound with an up-to-now unsolved structure. LiH₃As₂O₇ was also obtained from a mixture of Li₂CO₃, Fe₂O₃ and arsenic acid; in this case the crystals were accompanied by those of LiH₂As₃O₉. Efforts to synthesize these crystals from synthesis batches free of M^{3+} cations have failed so far. Such attempts have led to the formation of LiH₂As₃O₉ accompanied by LiAsO₃ (Driss & Jouini, 1989a).

KHAS₂O₆ formed colourless, translucent, thin tabular crystals from a dry mixture of K₂CO₃, Al₂O₃ and arsenic acid (volume ratio ca 2:1:4). Syntheses using Cr^{III}(NO₃)₃·9H₂O rather than Al₂O₃ lead to the same result. The same material could also be grown nearly phase-pure (yield ca 98%) from a mixture of K₂CO₃ and arsenic acid (volume ratio ca 1:4).

KH₃As₄O₁₂ was obtained from synthesis batches containing K₂CO₃, Ga₂O₃ and H₃AsO₄ (volume ratio ca 2:1:8), and in the equivalent Fe₂O₃-bearing mixture. Similarly, the isotopic

Table 2
Crystal data, data collection information and refinement details for the title compounds.

	KH ₃ As ₄ O ₁₂	KHAs ₂ O ₆	RbH ₃ As ₄ O ₁₂	LiH ₂ As ₃ O ₉
Crystal data				
Chemical formula	KH ₃ As ₄ O ₁₂	KHAs ₂ O ₆	RbH ₃ As ₄ O ₁₂	LiH ₂ As ₃ O ₉
<i>M_r</i>	533.80	285.95	580.17	377.72
Cell setting, space group	Triclinic, <i>P</i> $\bar{1}$	Monoclinic, <i>P</i> 2 ₁ / <i>c</i>	Triclinic, <i>P</i> $\bar{1}$	Monoclinic, <i>P</i> 2 ₁ / <i>n</i>
Temperature (K)	293 (2)	293 (2)	293 (2)	293 (2)
<i>a</i> , <i>b</i> , <i>c</i> (Å)	5.154 (1), 6.967 (1), 7.532 (2)	6.051 (1), 9.727 (2), 9.054 (2)	5.169 (1), 7.036 (1), 7.766 (2)	9.666 (2), 8.553 (2), 9.970 (2)
α , β , γ (°)	63.90 (3), 78.61 (3), 84.35 (3)	90.0, 94.21 (3), 90.0	63.31 (3), 79.87 (3), 84.38 (3)	90.0, 117.86 (3), 90.0
<i>V</i> (Å ³)	238.08 (11)	531.46 (18)	248.36 (11)	728.7 (3)
<i>Z</i>	1	4	1	4
<i>D_x</i> (Mg m ⁻³)	3.724	3.574	3.879	3.443
Radiation type	Mo <i>K</i> α	Mo <i>K</i> α	Mo <i>K</i> α	Mo <i>K</i> α
μ (mm ⁻¹)	14.42	13.31	18.27	13.70
Crystal form, colour	Tabular, colourless	Tabular–rhombohedral, colourless	Tabular, colourless	Large plate, colourless
Crystal size (mm)	0.04 × 0.03 × 0.02	0.12 × 0.10 × 0.08	0.17 × 0.13 × 0.05	0.15 × 0.08 × 0.08
Data collection				
Diffraction method	NoniusKappaCCD	NoniusKappaCCD	NoniusKappaCCD	NoniusKappaCCD
Data collection method	φ and ω scans	φ and ω scans	φ and ω scans	φ and ω scans
Absorption correction	Multi-scan (based on symmetry-related measurements)	Multi-scan (based on symmetry-related measurements)	Multi-scan (based on symmetry-related measurements)	Multi-scan (based on symmetry-related measurements)
<i>T_{min}</i>	0.596	0.298	0.147	0.233
<i>T_{max}</i>	0.761	0.416	0.462	0.407
No. of measured, independent and observed reflections	2699, 1385, 1188	3747, 1922, 1785	4335, 2190, 1995	5128, 2642, 2426
Criterion for observed reflections	<i>I</i> > 2σ(<i>I</i>)	<i>I</i> > 2σ(<i>I</i>)	<i>I</i> > 2σ(<i>I</i>)	<i>I</i> > 2σ(<i>I</i>)
<i>R_{int}</i>	0.018	0.011	0.026	0.012
θ_{\max} (°)	30.0	32.6	35.0	32.5
Refinement				
Refinement on	<i>F</i> ²	<i>F</i> ²	<i>F</i> ²	<i>F</i> ²
<i>R</i> [<i>F</i> ² > 2σ(<i>F</i> ²)], <i>wR</i> (<i>F</i> ²), <i>S</i>	0.024, 0.056, 1.12	0.017, 0.043, 1.12	0.028, 0.077, 1.04	0.017, 0.041, 1.13
No. of reflections	1385	1922	2190	2642
No. of parameters	88	87	88	127
H-atom treatment	Mixture of independent and constrained refinement	Refined independently	Mixture of independent and constrained refinement	Mixture of independent and constrained refinement
Weighting scheme	$w = 1/[\sigma^2(F_o^2) + (0.0232P)^2 + 0.3298P]$, where $P = (F_o^2 + 2F_c^2)/3$	$w = 1/[\sigma^2(F_o^2) + (0.0205P)^2 + 0.3321P]$, where $P = (F_o^2 + 2F_c^2)/3$	$w = 1/[\sigma^2(F_o^2) + (0.0495P)^2 + 0.1743P]$, where $P = (F_o^2 + 2F_c^2)/3$	$w = 1/[\sigma^2(F_o^2) + (0.0175P)^2 + 0.613P]$, where $P = (F_o^2 + 2F_c^2)/3$
(Δ/σ) _{max}	0.0001	0.001	<0.0001	0.001
$\Delta\rho_{\max}$, $\Delta\rho_{\min}$ (e Å ⁻³)	1.16, −0.69	0.71, −0.77	1.37, −1.59	0.67, −0.86
Extinction method	SHELXL97	SHELXL97	SHELXL97	SHELXL97
Extinction coefficient	0.0088 (14)	0.0092 (5)	0.059 (3)	0.0087 (3)
<hr/>				
	LiH ₃ As ₂ O ₇	CsAs ₃ O ₈	AgH ₂ As ₃ O ₉	
Crystal data				
Chemical formula	LiH ₃ As ₂ O ₇	CsAs ₃ O ₈	AgH ₂ As ₃ O ₉	
<i>M_r</i>	271.80	485.67	478.65	
Cell setting, space group	Monoclinic, <i>C</i> 2/ <i>m</i>	Monoclinic, <i>C</i> 2/ <i>c</i>	Triclinic, <i>P</i> $\bar{1}$	
Temperature (K)	293 (2)	293 (2)	293 (2)	
<i>a</i> , <i>b</i> , <i>c</i> (Å)	11.456 (2), 9.133 (2), 5.630 (1)	8.515 (2), 11.690 (2), 7.595 (2)	7.162 (1), 7.678 (2), 7.880 (2)	
α , β , γ (°)	90.0, 115.56 (3), 90.0	90.0, 112.70 (3), 90.0	110.72 (3), 106.47 (3), 105.43 (3)	
<i>V</i> (Å ³)	531.4 (2)	697.5 (3)	354.8 (2)	
<i>Z</i>	4	4	2	
<i>D_x</i> (Mg m ⁻³)	3.398	4.625	4.481	
Radiation type	Mo <i>K</i> α	Mo <i>K</i> α	Mo <i>K</i> α	
μ (mm ⁻¹)	12.55	19.44	16.75	
Crystal form, colour	Irregular fragment, colourless	Large strongly distorted octahedron, colourless–white	Dogtoothed-shaped, colourless	
Crystal size (mm)	0.08 × 0.07 × 0.06	0.10 × 0.08 × 0.07	0.15 × 0.13 × 0.08	
Data collection				
Diffraction method	NoniusKappaCCD	NoniusKappaCCD	NoniusKappaCCD	
Data collection method	φ and ω scans	φ and ω scans	φ and ω scans	
Absorption correction	Multi-scan (based on symmetry-related measurements)	Multi-scan (based on symmetry-related measurements)	Multi-scan (based on symmetry-related measurements)	

Table 2 (continued)

	LiH ₃ As ₂ O ₇	CsAs ₃ O ₈	AgH ₂ As ₃ O ₉
T_{\min}	0.433	0.247	0.188
T_{\max}	0.520	0.343	0.348
No. of measured, independent and observed reflections	1933, 1020, 924	3021, 1540, 1433	4992, 2568, 2375
Criterion for observed reflections	$I > 2\sigma(I)$	$I > 2\sigma(I)$	$I > 2\sigma(I)$
R_{int}	0.011	0.013	0.021
θ_{\max} (°)	32.6	34.9	32.5
Refinement			
Refinement on	F^2	F^2	F^2
$R[F^2 > 2\sigma(F^2)]$, $wR(F^2)$, S	0.017, 0.041, 1.14	0.020, 0.054, 1.03	0.029, 0.073, 1.09
No. of reflections	102	1540	2568
No. of parameters	61	57	127
H-atom treatment	Refined independently	No H atoms present	Mixture of independent and constrained refinement
Weighting scheme	$w = 1/[\sigma^2(F_o^2) + (0.017P)^2 + 0.9444P]$, where $P = (F_o^2 + 2F_c^2)/3$	$w = 1/[\sigma^2(F_o^2) + (0.0294P)^2 + 3.3231P]$, where $P = (F_o^2 + 2F_c^2)/3$	$w = 1/[\sigma^2(F_o^2) + (0.0459P)^2 + 0.211P]$, where $P = (F_o^2 + 2F_c^2)/3$
$(\Delta/\sigma)_{\max}$	<0.0001	<0.0001	0.001
$\Delta\rho_{\max}$, $\Delta\rho_{\min}$ (e Å ⁻³)	1.04, -0.54	2.18, -2.13	1.58, -2.35
Extinction method	<i>SHELXL97</i>	<i>SHELXL97</i>	<i>SHELXL97</i>
Extinction coefficient	0.0034 (3)	0.0076 (3)	0.068 (2)

Computer programs used: *COLLECT* (Nonius, 2002), *HKL DENZO* and *HKL SCALEPACK* (Otwinowski & Minor, 1997), *SHELXS97* (Sheldrick, 1997b), *SHELXL97* (Sheldrick, 1997a), *DIAMOND* (Brandenburg, 2005).

RbH₃As₄O₁₂ compound formed from mixtures of K₂CO₃, Sc₂O₃ [or Cr^{III}(NO₃)₃·9H₂O] and arsenic acid (volume ratio *ca* 2:1:4). RbH₃As₄O₁₂ was also grown from a mixture of K₂CO₃ and arsenic acid (volume ratio *ca* 1:4, yield *ca* 80%).

CsAs₃O₈ formed large white-to-colourless pseudo-octahedral crystals in a mixture of Cs₂CO₃, Fe₂O₃ and arsenic acid (volume ratio *ca* 1:1:4). The compound was accompanied by large pale bluish pseudo-octahedral crystals of CsFe₂-As(HAsO₄)₆ (Schwendtner & Kolitsch, 2007c), with a crystal structure derived from that of RbFe(HPO₄) (Lii & Wu, 1994). CsAs₃O₈ was also grown from a mixture of Cs₂CO₃ and arsenic acid (volume ratio *ca* 1:3, yield *ca* 70%). The material is hygroscopic and transforms in air within weeks into the novel compound Cs(H₂AsO₄)(H₃AsO₄)₂ (Schwendtner & Kolitsch, 2007d).

Colourless dogtooth-shaped to tabular (101) crystals of AgH₂As₃O₉ were grown from a mixture of Ag₂CO₃ and arsenic acid (volume ratio *ca* 1:3, yield *ca* 95%).

2.2. X-ray diffraction experiments and crystal structure solution

Several crystals of each of the seven compounds were selected for single-crystal studies with a Nonius KappaCCD single-crystal four-circle diffractometer [Mo tube, graphite monochromator, CCD detector frame size: 621 × 576 pixels (binned mode)], equipped with a 300 μm diameter capillary-optics collimator to provide increased resolution. A complete sphere of reciprocal space (φ and ω scans) was measured at room temperature for a suitable crystal of each compound (see Table 2 for details). The intensity data were processed with the Nonius program suite *DENZO-SMN* (Otwinowski & Minor, 1997) and corrected for Lorentz, polarization and background effects, and, by the multi-scan method (Otwinowski & Minor, 1997; Otwinowski *et al.*, 2003), for absorp-

tion. The crystal structures were solved with *SHELXS97* (Sheldrick, 1997b) and subsequent Fourier and difference Fourier syntheses, followed by anisotropic full-matrix least-squares refinements on F^2 using *SHELXL97* (Sheldrick, 1997a; Table 1). All H atoms could be detected and were successfully refined, in the cases of KH₃As₄O₁₂, RbH₃As₄O₁₂ and LiH₂As₃O₉ with restraints on the O—H bond distances [O—H = 0.90 (2) Å using the *SHELXL97 DFIX* command].

The crystals were of generally good quality and showed no signs of twinning. The last step of refinement resulted in final residuals $R1(F)$ of < 0.029 for all seven compounds (Table 2). All the largest residual peaks (electron densities 2.18/−2.13 e Å⁻³) in the final difference-Fourier map found for CsAs₃O₈ were close to the Cs positions, whereas the largest peaks for RbH₃As₄O₁₂ were close to O1 and As1. KHAs₂O₆ and LiH₂As₃O₉ did not show any distinct electron densities > |1| e Å⁻³; those of KH₃As₄O₁₂ and LiH₃As₂O₇ were only slightly larger (Table 2). Mean bond lengths and angles, calculated bond valences based on published parameters (Brown & Aldermatt, 1985) and distortion parameters of bond lengths (Brown & Shannon, 1973) and bond angles (Robinson *et al.*, 1971) for all As-centred polyhedra are presented in Table 3; hydrogen bonds are given in Table 4 and a detailed table of bond lengths and bond angles has been deposited as supplementary material.¹

3. Results and discussion

3.1. Crystal structure descriptions

All of the protonated new structure types are built up by the well known As₄O₁₄ cluster (Fig. 1), which was first described

¹ Supplementary data for this paper are available from the IUCr electronic archives (Reference: SN5044). Services for accessing these data are described at the back of the journal.

for $\text{BaH}_6\text{As}_4\text{O}_{14}$ (Blum *et al.*, 1977), or a derivative of that cluster, as is the case for CsAs_3O_8 . The cluster consists of two edge-sharing AsO_6 octahedra, the apices of both octahedra being connected on two sides *via* AsO_4 tetrahedra. In the following structures these clusters are either isolated and only connected by hydrogen bonds and the M^+ cations (as is the case for $\text{LiH}_3\text{As}_2\text{O}_7$) or they form chains as in $\text{KH}_3\text{As}_4\text{O}_{12}$, isotypic $\text{RbH}_3\text{As}_4\text{O}_{12}$ and $\text{AgH}_2\text{As}_3\text{O}_9$. Layer structures are formed by $\text{LiH}_2\text{As}_3\text{O}_9$ and KHAs_2O_6 , whereas in CsAs_3O_8 the clusters are reduced and polymerize to form a microporous framework.

3.1.1. Structure of $\text{LiH}_2\text{As}_3\text{O}_9$. In $\text{LiH}_2\text{As}_3\text{O}_9$ each As_4O_{14} cluster is corner-connected to four other clusters, thus forming a (101) layer (Fig. 2*a*). Additionally, the remaining unconnected two corners of the AsO_6 octahedra are shared with doubly protonated AsO_4 groups, which, as shown in Fig. 2(*b*), connect these layers *via* medium–strong to weak hydrogen bonds (Table 4). These H_2AsO_4 groups are also the main difference between this structure type and the related KHAs_2O_6 structure (see below), where the H_2AsO_4 groups are replaced by H atoms. $\text{LiH}_2\text{As}_3\text{O}_9$ and stoichiometrically identical $\text{AgH}_2\text{As}_3\text{O}_9$ (see §3.1.6) are the only ones of the title compounds that contain hydrogen but no protonated AsO_6 octahedra. The As–O distances are rather long for both tetrahedrally coordinated As atoms ($\langle \text{As1–O} \rangle = 1.694$, $\langle \text{As2–O} \rangle = 1.689$ Å) compared with the average distance for inorganic compounds of 1.682 Å (Baur, 1981). The longest As–O distances in both AsO_4 groups involve the O atoms corner-shared with the AsO_6 octahedra. This is explained by $\text{As}^{\text{V}}\text{–As}^{\text{V}}$ repulsion within the As_4O_{14} cluster, similar to the situation in diarsenates (long As– O_{bridge} distances). Still above average, but slightly shorter, are the As–OH distances, while the shortest distances are to the O atoms shared with the Li-centred polyhedra. The Li^+ cations are in [4 + 1] coordination [Li–O 1.958 (4)–2.072 (4) Å; the fifth distance is much larger at 2.643 (4) Å] and form edge-sharing dimers (Li_2O_6), not uncommon for inorganic Li compounds (Wenger & Armbruster, 1991). These dimers form – together with the H_2AsO_4 groups – a second layer sandwiched between two (101) octahedral–tetrahedral layers, and also connect the latter to a stable framework structure. The bond-valence sum (BVS) for Li is close to ideal with 0.97 v.u. (0.93 v.u. without the fifth O). The BVSs of the protonated O atoms are 1.19/1.36 as expected (Table 3, bottom), whereas the relatively low BVS of O1 (1.69 v.u.) can be explained by its role as acceptor of the strongest hydrogen bond (Table 4). The somewhat overbonded O2 (2.12 v.u.) shares relatively short bonds with two As atoms.

3.1.2. Structure of $\text{LiH}_3\text{As}_2\text{O}_7$. In this novel structure type the As_4O_{14} clusters are isolated, which is reflected by the high O/As ratio of 3.5. The Li^+ cations are four-coordinated [Li–O 1.985 (2)–1.993 (4) Å; BVS 0.97 v.u.] and form Li_2O_6 dimeric units as in $\text{LiH}_2\text{As}_3\text{O}_9$. These dimers corner-connect adjacent clusters along the *b* and *c* axes, thus forming (100) layer-like units (Fig. 3*a*). Adjacent layer-like units are offset by $b/2$, so that the HAsO_4 tetrahedra of the clusters can form bonds to the edge-sharing corners of the Li_2O_6 dimeric units, thereby

forming a stable framework (Fig. 3*a*). Additionally, two different hydrogen bonds reinforce the framework (Figs. 3*a* and *b*); the AsO_6 octahedron is diprotonated and forms medium–strong hydrogen bonds, whereas the HAsO_4 tetrahedron forms strong hydrogen bonds (Table 4). Interestingly, the shortest As–O distances of the H_2AsO_6 group are those to the protonated O with only 1.768 (1) Å, and also the average As–O distance of this polyhedron is rather short with 1.820 Å (mean $^{61}\text{As–O}$ distance is 1.830 Å, see discussion in §3.3 for details). The H_2AsO_6 polyhedron shows a slightly stronger distortion than that in $\text{LiH}_2\text{As}_3\text{O}_9$. The most underbonded O atoms are the donors of the hydrogen bonds; the low BVS of O5 (1.68 v.u.) can be explained by its role as an acceptor of a very strong hydrogen bond.

3.1.3. Structure of KHAs_2O_6 . This compound is isotypic to NaHAs_2O_6 (Nguyen Huy & Jouini, 1978) and is built up by As_4O_{14} clusters, which are corner-connected *via* their AsO_4 groups to interrupted (100) sheets, as in $\text{LiH}_2\text{As}_3\text{O}_9$ (*cf.* Figs. 2*a* and 4*a*). However, the connectivity between these zigzag sheets is different (*cf.* Figs. 2*b* and 4*b*); in KHAs_2O_6 the empty corners of both the AsO_6 octahedra of the cluster form hydrogen bonds which connect adjacent sheets, the seven-coordinated K^+ cations being located between two sheets, whereas in $\text{LiH}_2\text{As}_3\text{O}_9$ additional AsO_4 tetrahedra are sharing these corners and only these form the hydrogen bonds. The single hydrogen bond in KHAs_2O_6 is rather strong and is confirmed by the low BVS of the donor atom (O5, 1.22 v.u.). Again, the As–O distance to the protonated O atoms is the shortest one in the AsO_6 octahedron. The As–O distances in the AsO_4 group comprise one very short distance (involving the slightly underbonded O1 atom with 1.77 v.u., which is an acceptor of the hydrogen bond) and three nearly equally long bonds to the O atoms shared with the AsO_6 octahedra. In the first description of this structure type (Nguyen Huy & Jouini, 1978) the H atoms in NaHAs_2O_6 were not found, nor was the possible position of the H atom discussed. The mean bond length for the AsO_4 tetrahedra is slightly larger in NaHAs_2O_6

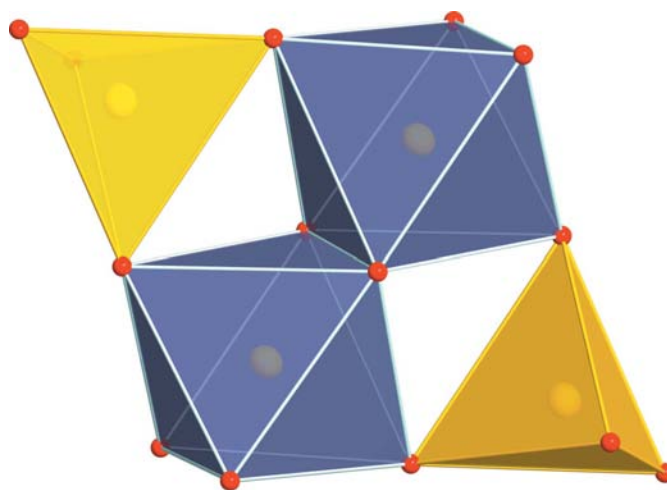


Figure 1

The As_4O_{14} cluster, which is the predominant building unit in AsO_6 -containing M^+ arsenates.

Table 3

Mean distances (Å) and angles (°), bond-valence sums and distortion parameters of the seven new title compounds.

Bond-length distortion (Brown & Shannon, 1973) for tetrahedra: $\Delta = \frac{1}{4} \sum_{i=1}^4 [(R_i - \bar{R})/\bar{R}]^2$; for octahedra: $\Delta = \frac{1}{6} \sum_{i=1}^6 [(R_i - \bar{R})/\bar{R}]^2$. Bond-angle distortion (Robinson *et al.*, 1971) for tetrahedra: $\sigma^2 = \sum_{i=1}^6 (\theta_i - 109.47^\circ)^2/5$; for octahedra: $\sigma^2 = \sum_{i=1}^{12} (\theta_i - 90^\circ)^2/11$.

	LiH ₂ As ₃ O ₉	LiH ₃ As ₂ O ₇	KHAs ₂ O ₆	KH ₃ As ₄ O ₁₂	RbH ₃ As ₄ O ₁₂	CsAs ₃ O ₈	AgH ₂ As ₃ O ₉						
As1													
$\langle^{[4]}\text{As1}-\text{O}\rangle$ (Å)	1.694	1.694	1.690	1.690	1.692	1.687	1.692						
BVS As1 (v.u.)	4.90	4.90	4.94	4.93	4.91	4.96	4.93						
Distortion (Δ)	4.48E-04	4.45E-04	2.97E-04	1.36E-04	1.18E-04	6.05E-06	5.92 E-06						
As2/3†													
$\langle^{[4]}\text{As2/3}-\text{O}\rangle$ (Å)	1.689						1.696						
BVS (v.u.)	4.95						4.87						
Distortion (Δ)	3.73E-04						4.29E-04						
As2/3†													
$\langle^{[6]}\text{As2/3}-\text{O}\rangle$ (Å)	1.822	1.821	1.828	1.831	1.830	1.835	1.824						
BVS (v.u.)	5.19	5.22	5.12	5.09	5.10	5.03	5.15						
Distortion (Δ)	1.38E-04	4.74E-04	4.84E-04	7.84E-04	7.42E-04	6.19E-04	1.01E-04						
As1													
$\langle\text{O}-^{[4]}\text{As1}-\text{O}\rangle$ (°)	109.22	109.27	109.35	109.44	109.44	109.41	109.38						
Distortion (σ ²)	43.85	24.13	31.91	5.91	5.89	15.39	38.42						
As2/3†													
$\langle\text{O}-^{[4]}\text{As2/3}-\text{O}\rangle$ (°)	109.18						109.30						
Distortion (σ ²)	47.58						35.09						
As2/3†													
$\langle\text{O}-^{[6]}\text{As2/3}-\text{O}\rangle$ (°)	90.02	90.04	90.03	89.98	90.02	90.12	90.02						
Distortion (σ ²)	7.87	21.38	40.21	8.55	9.11	24.64	35.09						
Bond-valence sums for O atoms (v.u.)													
O1	1.69	O1	1.92	O1	1.77	O1	2.07	O _H 1	1.48	O _H 1	1.44	O1	1.89
O2	2.12	O2	1.93	O2	2.12	O2	2.01	O2	2.14	O2	2.09	O _H 2	1.29
O3	1.96	O _H 3	1.14	O3	1.93	O3	1.87	O3	1.87	O3	1.87	O3	1.69
O4	1.91	O _H 4	1.24	O4	2.03	O4	2.15	O4	2.03	O4	2.04	O4	2.05
O5	1.92	O5	1.68	O _H 5	1.20	O _H 5	1.22	O _H 5	1.27	O5		O5	1.86
O _H 6	1.19			O6	1.81	O6	1.96	O6	1.83			O6	2.01
O _H 7	1.36											O _H 7	1.27
O8	2.09											O8	1.95
O9	1.78											O9	1.93

† The second AsO₄ polyhedron in LiH₂As₃O₉ is numbered As2, whereas it is numbered As3 in AgH₂As₃O₉; the AsO₆ polyhedra are numbered As2 in all compounds except LiH₂As₃O₉, where it is called As3.

than in KHAs₂O₆ (1.70 *versus* 1.690 Å), whereas the opposite is true for the AsO₆ octahedra (1.82 *versus* 1.831 Å). KHAs₂O₆ clearly is a sheet structure, whereas the related LiH₂As₃O₉ structure can also be regarded as a framework if the LiO₄ tetrahedra are considered as part of the framework.

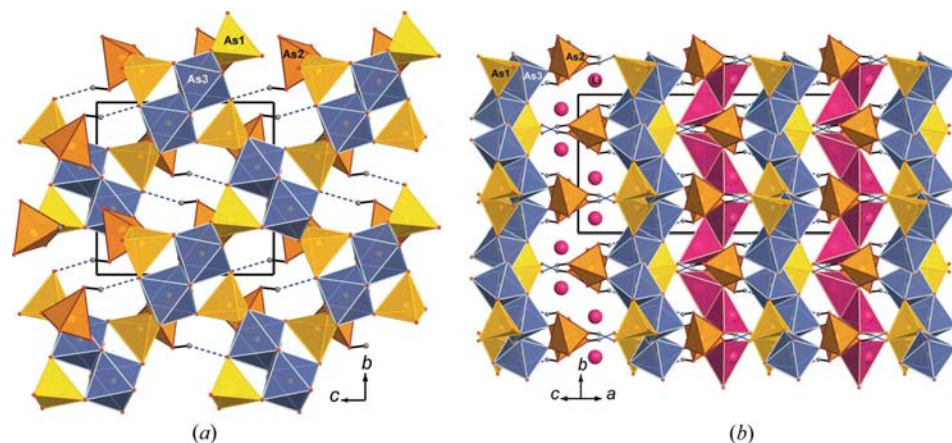


Figure 2

LiH₂As₃O₉: (a) view along [100], documenting the connectivity within the (100) octahedral-tetrahedral layer; (b) view along [101], showing the sequence of octahedral-tetrahedral layers and layers containing H₂AsO₄ and Li₂O₆ dimers (Li⁺ cations shown in left part of figure).

3.1.4. Structures of KH₃As₄O₁₂ and RbH₃As₄O₁₂. In these two new compounds, representing a novel structure type, the sheet structure of KHAs₂O₆ is broken up into chains. The As₄O₁₄ clusters are corner-linked *via* the AsO₄ tetrahedra to form infinite chains parallel to the *a* axis. All the empty corners of both AsO₆ octahedra and AsO₄ tetrahedra are protonated and involved in hydrogen bonds. The resulting network provides reinforcement along the *b* and *c* axes (Fig. 5a). Unlike KHAs₂O₆, where the hydrogen donor belongs to the AsO₆ octahedron and the acceptor to AsO₄, here a medium-strong hydrogen bond exists between two AsO₆ groups and a very strong, symmetry-restricted hydrogen bond involving a characteristically split half-occupied H position between two AsO₄ groups [O1—H₂...O1 2.453 (4)/2.458 (5) Å for the Rb and K compounds, respectively]. The shortest As—O bonds

Table 4
Hydrogen bonds of the six new protonated M^+ arsenates.

Compound	$D-H$	$d(D-H)$ (Å)	$d(H \cdots A)$ (Å)	$\angle DHA$ (°)	$d(D \cdots A)$ (Å)	A
LiH ₂ As ₃ O ₉	O6–H1	0.877 (19)	2.11 (3)	157 (4)	2.936 (2)	O4
	O7–H2†	0.86 (4)	1.85 (4)	161 (3)	2.676 (2)	O1
LiH ₃ As ₂ O ₇	O4–H1†	0.74 (3)	2.11 (3)	174 (3)	2.8410 (19)	O3
	O3–H2†	0.68 (5)	1.87 (5)	171 (5)	2.552 (2)	O5
KHAs ₂ O ₆	O5–H1†	0.77 (3)	1.91 (3)	167 (3)	2.6669 (18)	O1
KH ₃ As ₄ O ₁₂	O5–H1	0.885 (14)	1.949 (19)	164 (4)	2.810 (3)	O3
	O1–H2	0.89 (2)	1.58 (2)	166 (7)	2.458 (5)	O1
RbH ₃ As ₄ O ₁₂	O5–H1	0.852 (19)	1.98 (2)	169 (4)	2.822 (3)	O3
	O1–H2	0.901 (10)	1.58 (3)	161 (8)	2.453 (4)	O1
AgH ₂ As ₃ O ₉	O2–H1†	0.879 (19)	1.70 (2)	162 (5)	2.551 (4)	O3
	O7–H2	0.87 (6)	1.97 (7)	157 (6)	2.796 (3)	O6

† Not restrained

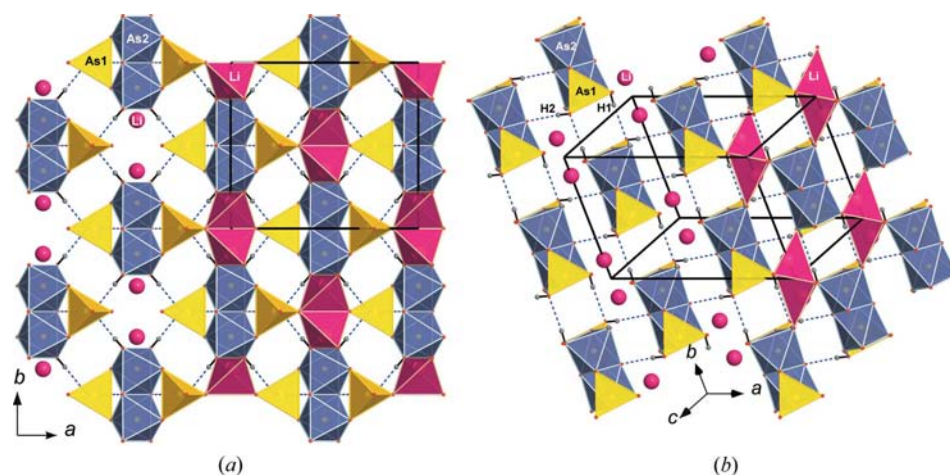


Figure 3
LiH₃As₂O₇: (a) view along c , showing isolated As₄O₁₄ clusters; (b) view along $[112]$ showing hydrogen-bonding scheme. The Li⁺ cations are partly shown as polyhedra in both pictures.

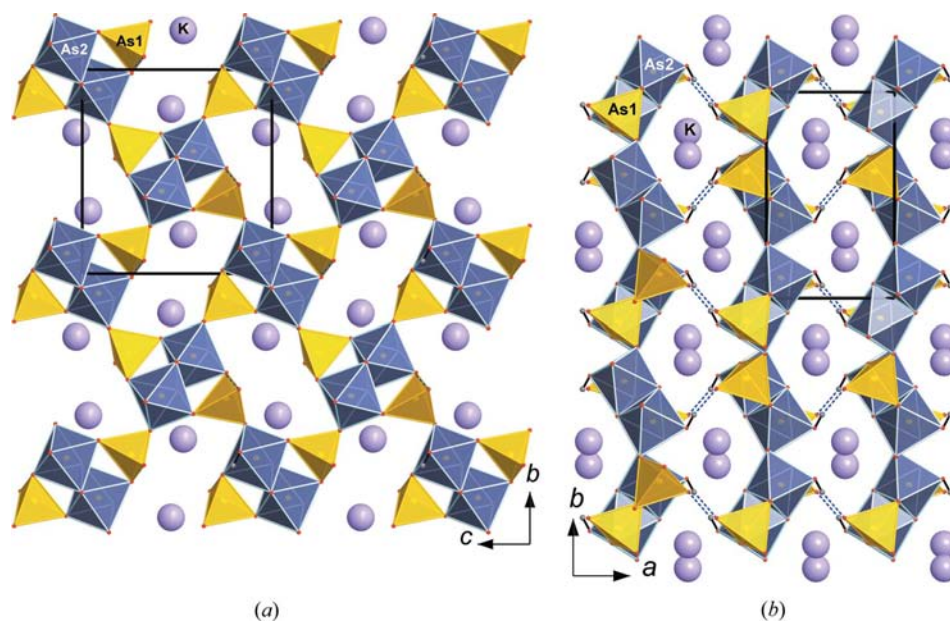


Figure 4
KHAs₂O₆: (a) view along a and connectivity of As₄O₁₄ clusters to (100) sheets (*cf.* Fig. 2a); (b) view along c and connection between sheets, with K atoms in voids (*cf.* Fig. 2b).

of the AsO₄ and AsO₆ polyhedra of both compounds involve the protonated O atom, whereas the longest bonds are to the bridging O atoms of the other arsenate groups. The K/Rb atoms are located in (100) planes, separating the chains. They have a rather large, irregular coordination sphere comprising ten oxygen ligands. The average Rb–O distance of 3.07 Å is close to the expected value of *ca* 3.03 Å (Khan & Baur, 1972) and only slightly longer than the corresponding distance of the K⁺ cation ($\langle K-O \rangle = 2.99$ Å). Owing to these slight differences in the mean bond lengths the BVS is rather large for the Rb atom (1.21 v.u.), but as expected for the K atom (1.01 v.u.).

3.1.5. Structure of CsAs₃O₈.

The structure of CsAs₃O₈ is the most unusual among the title compounds because it is a rather condensed framework structure. It can most easily be described as being built up by As₃O₁₂ rings (visualized as an As₄O₁₄ cluster with one AsO₄ tetrahedron missing). These rings share edges with AsO₆ octahedra of two adjacent rings to form infinite zigzag AsO₆ chains running parallel to $[100]$ (Fig. 6a). The chains are firmly connected to each other by AsO₄ tetrahedra (Figs. 6b and c), thus forming a rather dense framework structure with the lowest O/As ratio (2.67) of all known M^+ arsenates(V) containing arsenic in octahedral coordination. Nevertheless, it represents a microporous structure type with ten-coordinated Cs cations located at the intersections of channels parallel to $[110]$ and $[001]$ ($\langle Cs-O \rangle = 3.300$ Å). As every AsO₄ tetrahedron shares its corners with four AsO₆ octahedra and each AsO₆ octahedron shares edges with two other symmetry-equivalent AsO₆ octahedra and corners with two different AsO₄ tetrahedra, there is no room for hydrogen bonds. As expected for four identical ligand atoms, the As–O bond lengths of AsO₄ are very similar and the bond-length distortion is also rather low, unlike all six other compounds where there is at least one very short and a few very long As–O bonds (see supplementary

table). The mean $^{41}\text{As}-\text{O}$ bond length (1.687 Å) is still above the average 1.682 Å (Baur, 1981), but considerably shorter than in the other compounds. The longest As—O bond lengths in the AsO_6 octahedra are the ones to O atoms shared with the AsO_4 tetrahedra, as can be expected by the stronger influence of the As^{V} atom in this cation, compared with that in the AsO_6 octahedra. The stoichiometry of this compound is so far unprecedented among the M^+ arsenates discussed herein.

3.1.6. Structure of $\text{AgH}_2\text{As}_3\text{O}_9$. This structure type is isotopic to that of $\text{NaH}_2\text{As}_3\text{O}_9$ (Driss, Jouini, Durif & Averbuch-Pouchot, 1988). Its sum formula is similar to $\text{LiH}_2\text{As}_3\text{O}_9$, but the structure types are not related. Both types are built up by As_4O_{14} units, but where those are connected to layers in

$\text{LiH}_2\text{As}_3\text{O}_9$, they are connected by two AsO_4 groups to infinite chains parallel to a (Figs. 7a and b) in $\text{AgH}_2\text{As}_3\text{O}_9$. The H atoms very firmly connect these chains in directions b and c through strong to medium–strong hydrogen bonds (Table 4). The Ag cation is six-coordinated as is the Na^+ cation in the isotopic Na compound and the AgO_6 polyhedron can be best described as a strongly distorted octahedron ($\Delta = 0.0041$, Brown & Shannon, 1973; $\sigma^2 = 228.2$, Robinson *et al.*, 1971; mean Ag—O = 2.515 Å compared with 2.435 Å in the Na compound). The As—O bond lengths in AsO_4 tetrahedra are both longer (1.692 and 1.696 Å) than the literature values (Baur, 1981) and are longest for the tetrahedron of the As_4O_{14} cluster. This pattern is similar to the situation in the isotopic

Na compound, where the differences between As1 and As3 are even more pronounced. As expected from the larger ionic radius of six-coordinated Ag^+ compared with Na^+ (Shannon, 1976), the cell volume of the new compound $\text{AgH}_2\text{As}_3\text{O}_9$ is larger than that of $\text{NaH}_2\text{As}_3\text{O}_9$ (Table 1). Cell lengths b and c are elongated in the Ag compound, whereas the a cell length is slightly shorter than in the Na compound. This can be explained by the arrangement of the $[\text{H}_2\text{As}_3\text{O}_9]^-$ chains in the structure: These chains run parallel to a ; this cell parameter is therefore hardly influenced by the size of the M^+ cation.

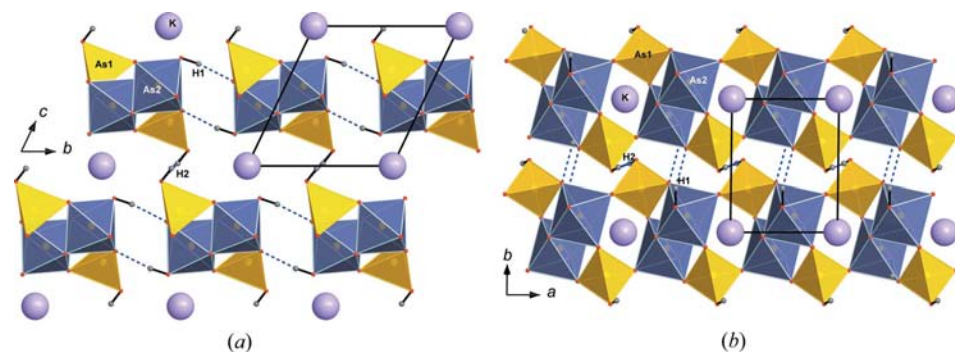


Figure 5
 $\text{KH}_3\text{As}_4\text{O}_{12}$: (a) view parallel to infinite chains extending parallel to a , showing linkage between chains via hydrogen bonds (note the split H2 position); (b) view along c , perpendicular to chains, showing the connectivity of the chains.

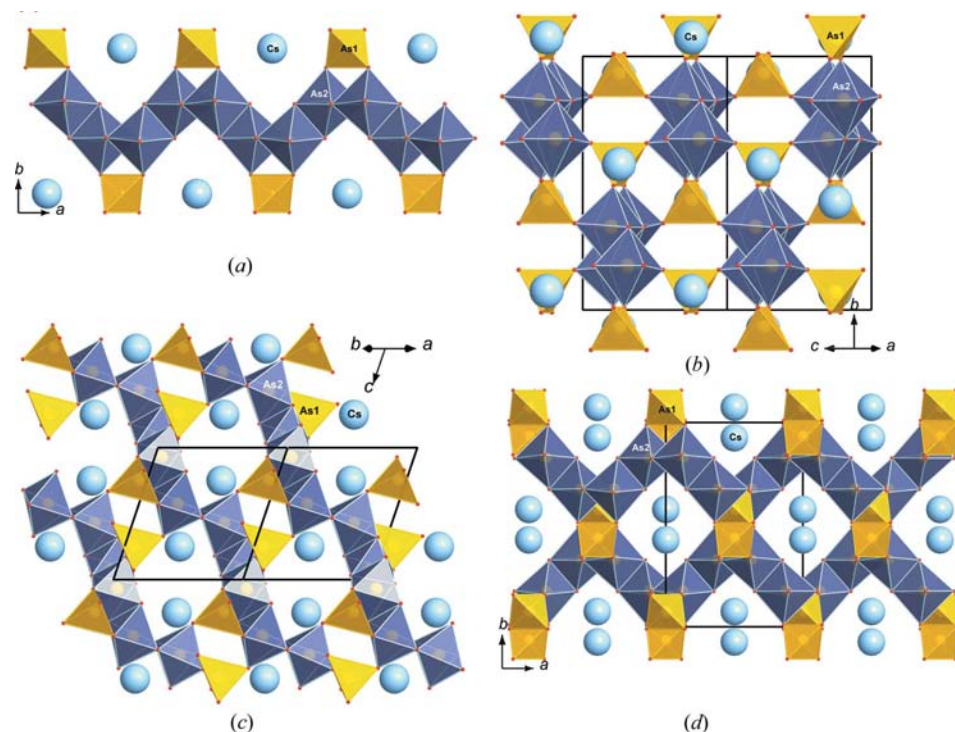


Figure 6
 CsAs_3O_8 : (a) view along c showing zigzag AsO_6 chains running parallel to a ; (b) view along $[101]$ demonstrating connection between the chains via AsO_4 tetrahedra; (c) view along $[110]$ with Cs-filled microporous channels; (d) view along $[001]$ with Cs-filled microporous channels.

3.2. Comparison and discussion of all 15 structure types containing As in octahedral coordination

Comparing the seven novel compounds to the eight other known compounds containing M^+ cations and arsenic(V) in octahedral coordination (Table 1) demonstrates that six different building units are present; the most prevalent is the As_4O_{14} cluster, which is encountered in 10 of the 15 compounds. In these structure types, every AsO_6 octahedron shares only one edge with another AsO_6 octahedron. The connectivity between the As_4O_{14} units is the main difference in these ten compounds. $\text{Ag}_4\text{H}_4\text{As}_4\text{O}_{14}$ (Boudjada & Averbuch-Pouchot, 1984), $\text{Na}_3\text{H}_5\text{As}_4\text{O}_{14}$ (Driss & Jouini, 1989b) and the novel $\text{LiH}_3\text{As}_2\text{O}_7$ all represent structures with

isolated As_4O_{14} groups. Connectivity between the groups is provided through the M^+ cations and hydrogen bonds. Their structures and stoichiometries are different. For every As_4O_{14} unit the ratio of $\text{H}:M^+$ differs in these three compounds and is largest (3) in the Li compound and smallest (1) in the Ag compound. The influence of the hydrogen bonds reinforcing the structure is therefore more pronounced in the Li compound, whereas the M^+ cations play a more important part in the Ag compound. $\text{Na}_3\text{H}_5\text{As}_4\text{O}_{14}$ lies somewhere in-between. The two structure types $M^+\text{H}_2\text{As}_3\text{O}_9$ ($M^+ = \text{Na}, \text{Ag}$) and $M^+\text{H}_3\text{As}_4\text{O}_{14}$ ($M^+ = \text{K}, \text{Rb}$) are both chain structures; the As_4O_{14} groups are linked to infinite chains *via* the AsO_4 groups of the cluster. The difference arises through the connectivity of the chains, which is directly through hydrogen bonds in the $M^+\text{H}_3\text{As}_4\text{O}_{14}$ structure, whereas additional AsO_4 groups attached to the cluster connect adjacent chains through hydrogen bonds in the $M^+\text{H}_2\text{As}_3\text{O}_9$ -type structure ($M^+ = \text{Na}, \text{Ag}$). This fact is also the main difference in the two sheet-structure types $M^+\text{HAS}_2\text{O}_6$ ($M^+ = \text{Na}, \text{K}$) and $\text{LiH}_2\text{As}_3\text{O}_9$, where the As_4O_{14} groups link to sheets through the AsO_4 groups of the cluster. However, connectivity between adjacent sheets is only achieved through hydrogen bonds in the $M^+\text{HAS}_2\text{O}_6$ type and *via* an additional AsO_4 group, that forms hydrogen bonds, in the $\text{LiH}_2\text{As}_3\text{O}_9$ -type structure.

The following five structure types do not contain As_4O_{14} groups. The building unit of CsAs_3O_8 consists of infinite zigzag chains of edge-sharing AsO_6 octahedra; therefore, every AsO_6 shares two edges with two more AsO_6 octahedra. This is taken a step further in the recently described, oxygen-deficient $\text{Na}_7\text{As}_{11}\text{O}_{31}$ (Guesmi *et al.*, 2006), where some of the octahedra share edges with two neighbouring AsO_6 groups and the others have three common edges with other AsO_6 groups. $\text{Na}_7\text{As}_{11}\text{O}_{31}$ can therefore be considered the missing link between CsAs_3O_8 and LiAsO_3 (Driss & Jouini, 1989a). In the latter the structure is built up by sheets of edge-sharing AsO_6 octahedra, and each AsO_6 group shares edges with three neighbouring AsO_6 groups. This structure type is also the only one based solely on octahedrally coordinated arsenic. With respect to edge connections of the AsO_6 unit the structure of

AgAsO_3 (Curda *et al.*, 2004) is probably the most unusual, as it represents the only type based on infinite chains of corner- (instead of edge-) sharing AsO_6 octahedra, which are linked by AsO_4 tetrahedra, similar to the As_4O_{14} clusters. The structure type of $\text{Na}_2\text{As}_4\text{O}_{11}$ (Driss, Jouini & Omezzine, 1988) can be seen as the link between the AgAsO_3 structure and those structures based solely on edge-sharing AsO_6 polyhedra. It consists of two edge-sharing AsO_6 octahedra which are linked through a common corner to infinite chains. These chains are connected by AsO_4 tetrahedra to a framework structure.

The chemical formula of the M^+ arsenates gives, analogous to silicates, some indication about the polymerization of the As_4O_{14} cluster units. The O/As ratio is highest for the isolated clusters (3.5), medium for chain- and layer-structures (3) and lowest for framework structures (< 3), as expected. The same applies for the H/As ratio, which is highest in structure types with isolated As-based clusters and, with increasing polymerization, decreases down to zero for the framework structures (*e.g.* CsAs_3O_8). The oxygen-deficient $\text{Na}_7\text{As}_{11}\text{O}_{31}$ is the only type that does not completely obey this rule.

Unlike other protonated arsenates, where $\text{As}-\text{OH}$ distances are usually longer than $\text{As}-\text{O}$ distances ($\langle \text{As}-\text{OH} \rangle = 1.731 \text{ \AA}$; Ferraris & Ivaldi, 1984), the exact opposite is encountered in the present structure types. The strong influence of the As^{V} atom with its strong covalent bonds results in a competition for the shared O atoms. This can be seen very easily in all protonated AsO_4 tetrahedra, where the $\text{As}-\text{OH}$ distances are usually a lot shorter than average, while the bonds between As atoms and O atoms shared with other As atoms are significantly longer, as expected from As-As repulsion (see supplementary table). It would be expected that this influence is stronger if AsO_4 tetrahedra (instead of AsO_6 octahedra) are involved as ligands and indeed this is very clearly the case as shown in CsAs_3O_8 . The average $\text{As}-\text{O}$ bond lengths of all AsO_4 tetrahedra in these arsenates are above the average value of 1.682 \AA (Baur, 1981) and range between 1.687 and 1.696 \AA . It is interesting to note that a rather large average $\text{As}-\text{O}$ distance occurs in the Li

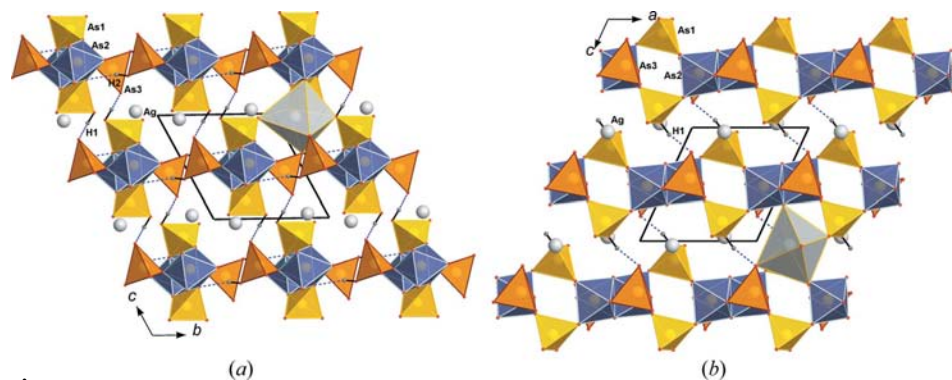


Figure 7
 $\text{AgH}_2\text{As}_3\text{O}_9$: (a) view along $[100]$, documenting the existence of chains, connected *via* hydrogen bonds and octahedrally coordinated Ag^+ cations, running parallel to \mathbf{a} ; (b) view along $[010]$, showing the chains consisting of As_4O_{14} groups connected *via* the As_1O_4 groups. The chains are connected *via* hydrogen bonds of As_3O_4 groups. Both figures contain an additional single polyhedral representation of the AgO_6 polyhedron.

compounds, whereas the smallest average distance can be observed in the Cs compound. Exactly the opposite is true for the AsO_6 octahedra, where the average $\text{As}-\text{O}$ distances range between 1.821 ($\text{LiH}_3\text{As}_2\text{O}_7$) and 1.835 \AA (CsAs_3O_8). This can at least partly be explained by the different ligands. In the case of Cs the only slightly distorted AsO_4 tetrahedron leads to a smaller average bond length, in agreement with the distortion theorem (Brown & Shannon, 1973; Brown, 1981); on the other hand, the linkage of the AsO_6 octahedra with six different As atoms does not considerably

change its distortion values, but leads to an increase of the mean bond length through the above described influences of the As^V cation (As–As repulsion). For unknown reasons not a single one of the 15 (NH₄) arsenates in the ICSD database contains arsenic in octahedral coordination and our studies of this system have not yielded any new NH₄–^[6]As compounds so far.

3.3. Bond-length distribution in AsO₆ octahedra

An analysis of all As–O bond lengths in AsO₆-containing arsenates available in the ICSD was conducted. Structures fulfilling the following requirements were considered: refined structure, conventional *R* factor < 0.072, coordination spheres comprise exactly six O atoms, no partial substitution of the As or O atoms. All in all, only 24 AsO₆ polyhedra belonging to 23 different compounds in the ICSD database meet these conditions. Together with the seven new compounds and the recently described Na₇As₁₁O₃₁ (Guesmi *et al.*, 2006), 33 AsO₆ octahedra of 31 compounds (four of these have *R* values > 5) fulfil the requirements and were used for the analysis. It is worth noting that there are more than 900 AsO₄ polyhedra that meet similar requirements – AsO₆ polyhedra therefore occur only in less than 3% of all arsenates (Schwendtner, 2007). Besides the 15 *M*⁺ arsenate compounds listed in Table 1 the following compounds were used: BaH₆As₄O₁₄ (Blum *et al.*, 1977); Mg_{8.5}(AsO₄)₂(AsO₆)O₂ (Bless & Kostiner, 1973); Ni_{8.5}(AsO₄)₂(AsO₆)O₂ (Fleet & Barbier, 1989); K₇(AsV₁₄O₄₀)(H₂O)₁₂ (Mueller *et al.*, 1991); Co₅(AsVO₁₀) (Osterloh & Müller-Buschbaum, 1994); Ni(AsO₃)₂, Co(AsO₃)₂ and Mn(AsO₃)₂ (Nakua & Greedan, 1995); Pb(As₂O₆) and Ca(As₂O₆) (Losilla *et al.*, 1995); Cd(As₂O₆) (Weil, 2001); Hg(As₂O₆) (Mormann & Jeitschko, 2000); Hg₂(As₂O₆) and Hg(As₂O₆) (Weil, 2000); As₂O₅ (Jansen, 1978); AsPO₅ (Jansen *et al.*, 1992). The As–O distances in the structures available in the ICSD were directly calculated using ICSD software; only Na₂As₄O₁₁ (Driss, Jouini & Omezzine, 1988) showed inconsistencies. The bond lengths in the paper differ considerably from that of the ICSD, which is astonishing since the atomic coordinates are identical in both instances (obviously there must be some error in the atomic coordinates given in the paper) – therefore the distances given in the paper were used for analysis.

The mean As–O distance in these 33 polyhedra is 1.830 (2) Å. The distances range between 1.736 and 1.918 Å for individual As–O distances and from 1.811 to 1.857 Å for average distances of the 33 individual polyhedra. This is somewhat shorter than expected as it gives a mean BVS of 5.08 (2) v.u. for all used AsO₆ octahedra. A thorough discussion of all AsO₄ and AsO₆ polyhedra in inorganic arsenate compounds will be published separately (Schwendtner, 2007).

4. Conclusions

AsO₆ is a very uncommon coordination polyhedron in As^V compounds, but compared with other As^V-bearing compounds

it is rather common among *M*⁺ arsenates and to a lesser extent among *M*²⁺ arsenates.

More than 20% of all AsO₆-bearing compounds (*R* < 0.08) are described in this paper for the first time. All of them were synthesized under mild hydrothermal conditions without added water (basically from a melt of arsenic acid). All the compounds listed in Table 1 were also grown by relatively mild conditions between 773 K (AgAsO₃; Curda *et al.*, 2004) and room temperature (Ag₄H₄AsO₁₄; Boudjada & Averbuch-Pouchot, 1984). As with the new compounds the absence of H₂O (Curda *et al.*, 2004) was noted to be crucial. This might suggest that the more prevalent high-temperature solid-state reactions or hydrothermal conditions containing H₂O are less suited for the growth of AsO₆-bearing compounds, although high-temperature synthesis (chemical transport reaction at 993 K) has been successful in the case of Cd(As₂O₆) (Weil, 2001) for example. In general, high coordination numbers seem to be less common at higher temperatures. Therefore, the number of octahedrally coordinated As atoms is likely to increase significantly if the following two conditions are adhered to during synthesis: mild temperatures and high concentration of arsenic (no dilution with H₂O).

Financial support by a DOC FFORTE fellowship of the Austrian Academy of Sciences (ÖAW) to K. Schwendtner is gratefully acknowledged. We thank one of two anonymous referees and Co-editor van Smaalen for very helpful comments.

References

- Baran, E. J., Schwendtner, K. & Kolitsch, U. (2006a). *J. Raman Spectrosc.* **37**, 1335–1340.
- Baran, E. J., Schwendtner, K. & Kolitsch, U. (2006b). *J. Raman Spectrosc.* **37**, 1453–1455.
- Baur, W. H. (1981). *Interatomic Distance Predictions for Computer Simulation of Crystal Structures*. New York: Academic Press.
- Bless, P. W. & Kostiner, E. (1973). *J. Solid State Chem.* **6**, 80–85.
- Blum, D., Durif, A. & Guitel, J. C. (1977). *Acta Cryst.* **B33**, 3222–3224.
- Boudjada, A. & Averbuch-Pouchot, M. T. (1984). *J. Solid State Chem.* **51**, 76–82.
- Brandenburg, K. (2005). *DIAMOND*, Version 3.1a. Bonn, Germany.
- Brown, I. D. (1981). *Structure and Bonding in Crystals*, edited by M. O'Keeffe & A. Navrotsky, Vol. II, pp. 1–30. New York: Academic Press.
- Brown, I. D. & Aldermatt, D. (1985). *Acta Cryst.* **B41**, 244–247.
- Brown, I. D. & Shannon, R. D. (1973). *Acta Cryst.* **A29**, 266–282.
- Curda, J., Peters, E. M. & Jansen, M. (2004). *Z. Anorg. Allg. Chem.* **630**, 491–494.
- Driss, A. & Jouini, T. (1989a). *J. Solid State Chem.* **78**, 126–129.
- Driss, A. & Jouini, T. (1989b). *J. Solid State Chem.* **78**, 130–135.
- Driss, A., Jouini, T., Durif, A. & Averbuch-Pouchot, M. T. (1988). *Acta Cryst.* **C44**, 1507–1510.
- Driss, A., Jouini, T. & Omezzine, M. (1988). *Acta Cryst.* **C44**, 788–791.
- Ferraris, G. & Ivaldi, G. (1984). *Acta Cryst.* **B40**, 1–6.
- Fleet, M. E. & Barbier, J. (1989). *Acta Cryst.* **B45**, 201–205.
- Guesmi, A., Nespolo, M. & Driss, A. (2006). *J. Solid State Chem.* **179**, 2433–2438.
- Jansen, M. (1978). *Z. Anorg. Allg. Chem.* **441**, 5–12.
- Jansen, M., Begemann, B. & Geb, J. (1992). *Z. Anorg. Allg. Chem.* **610**, 139–144.
- Khan, A. A. & Baur, W. H. (1972). *Acta Cryst.* **B28**, 683–693.

- Kolitsch, U. (2004). *Z. Kristallogr. New Cryst. Struct.* **219**, 207–208.
- Kolitsch, U. & Schwendtner, K. (2004). *Z. Kristallogr. New Cryst. Struct.* **219**, 347–348.
- Kolitsch, U. & Schwendtner, K. (2005). *Acta Cryst.* **C61**, i86–i98.
- Lii, K.-H. & Wu, L.-S. (1994). *J. Chem. Soc. A*, **10**, 1577–1580.
- Losilla, E. R., Aranda, M. A. G., Ramirez, F. J. & Bruque, S. (1995). *J. Phys. Chem. A*, **99**, 12975–12979.
- Mormann, T. J. & Jeitschko, W. (2000). *Z. Kristallogr. New Cryst. Struct.* **215**, 471–472.
- Mueller, A., Doering, J., Ishaque Khan, M. & Wittneben, V. (1991). *Angew. Chem.* **103**, 203–205.
- Nakua, A. M. & Greedan, J. E. (1995). *J. Solid State Chem.* **118**, 402–411.
- Nguyen Huy, D. & Jouini, T. (1978). *Acta Cryst.* **B34**, 3727–3729.
- Nonius, BV (2002). *COLLECT*. Nonius BV, Delft, The Netherlands.
- Osterloh, D. & Müller-Buschbaum, H. (1994). *Z. Anorg. Allg. Chem.* **620**, 319–322.
- Otwinowski, Z., Borek, D., Majewski, W. & Minor, W. (2003). *Acta Cryst.* **A59**, 228–234.
- Otwinowski, Z. & Minor, W. (1997). *Methods Enzymol.* **276**, 307–326.
- Robinson, K., Gibbs, G. V. & Ribbe, P. H. (1971). *Science*, **172**, 567–570.
- Schwendtner, K. (2006). *J. Alloys Compd.* **421**, 57–63.
- Schwendtner, K. (2007). In preparation.
- Schwendtner, K. & Kolitsch, U. (2004a). *Acta Cryst.* **C60**, i79–i83.
- Schwendtner, K. & Kolitsch, U. (2004b). *Acta Cryst.* **C60**, i84–i88.
- Schwendtner, K. & Kolitsch, U. (2005a). *Acta Cryst.* **C61**, i90–i93.
- Schwendtner, K. & Kolitsch, U. (2005b). *Mitt. Österr. Mineral. Ges.* **151**, 109.
- Schwendtner, K. & Kolitsch, U. (2005c). *Mitt. Österr. Mineral. Ges.* **151**, 110.
- Schwendtner, K. & Kolitsch, U. (2007a). *Acta Cryst.* **C63**, i17–i20.
- Schwendtner, K. & Kolitsch, U. (2007b). *Eur. J. Mineral.* Accepted for publication.
- Schwendtner, K. & Kolitsch, U. (2007c). To be submitted.
- Schwendtner, K. & Kolitsch, U. (2007d). In preparation.
- Schwendtner, K., Kolitsch, U. & Tillmanns, E. (2006a). 15th Slovenian–Croatian Crystallographic Meeting, p. 36. Jezersko, Slovenia.
- Schwendtner, K., Kolitsch, U. & Tillmanns, E. (2006b). 19th General Meeting of the International Mineralogical Association, p. 90387. Kobe, Japan.
- Schwendtner, K., Kolitsch, U. & Tillmanns, E. (2006c). *Z. Kristallogr. Suppl.* **24**, 119.
- Shannon, R. D. (1976). *Acta Cryst.* **A32**, 751–767.
- Sheldrick, G. M. (1997a). *SHELXL97*. University of Göttingen, Germany.
- Sheldrick, G. M. (1997b). *SHELXS97*. University of Göttingen, Germany.
- Weil, M. (2000). *Z. Naturforsch. Teil B*, **55**, 699–706.
- Weil, M. (2001). *Acta Cryst.* **E57**, i22–i23.
- Wenger, M. & Armbruster, T. (1991). *Eur. J. Mineral.* **3**, 387–399.